Structure and Properties of Injection-Molded Polypropylenes with Different Molecular Weight Distribution and Tacticity Characteristics

MITSUYOSHI FUJIYAMA, YOSHIYUKI KITAJIMA, HITOSHI INATA

Tokuyama Research Laboratory, Tokuyama Corp., 1-1, Harumi-cho, Tokuyama-shi, Yamaguchi-ken, 745-0024 Japan

Received 17 May 2001; accepted 26 July 2001

ABSTRACT: Two series of polypropylenes with different molecular weight distribution and tacticity characteristics were injection molded into flexural test specimens by varying cylinder temperature and the effects of the molecular weight distribution and tacticity on the structure and properties of the moldings were studied. Measured propertied were flexural modulus, flexural strength, heat distortion temperature, Izod impact strength, and mold shrinkage and structures studied were crystallinity, the thickness of skin layer, a*-axis-oriented component fraction and crystalline orientation functions. The relations between the structures and properties were also studied. It was found that the molecular weight distribution and tacticity characteristics affect the properties mainly through the molecular orientation and crystallinity, respectively.
 J Appl Polym Sci 84: 2142–2156, 2002

Key words: poly(propylene); molecular weight distribution; injection molding; crystallization; orientation

INTRODUCTION

The Ziegler-Natta catalyst for polyolefins has been actively studied from both scientific and industrial aspects for about 45 years since its discovery. This made progress in the manufacturing processes and qualities of polyethylene and polypropylene (PP).

Particularly for the PP catalyst, the early $TiCl_3$-type catalyst has been improved to the $MgCl_2$-supported titanium catalyst, which has largely improved the activity of polymerization and the tacticity of polymer. As a result, the PP manufacturing process has been simplified from the deashing and washing process to the nondeashing and nonwashing process, and further to the ultimate gas-phase process. At the same time, the quality of polymer has also been made an improved step, leading to industrial production of PPs with high tacticity and crystallinity.

The difference between PPs prepared by the $MgCl_2$-supported titanium catalyst and the $TiCl_3$-type catalyst is that the former shows higher tacticity and narrower molecular weight distribution than the latter, which is assumed to affect the quality such as the processing and product properties.

In our previous article,[1] both series of PPs have been clarified in the molecular weight distribution and rheological characteristics intimately related to the processing properties. In the present article, we aimed to clarify the structure and properties of injection moldings of both series of PPs.

As for properties, mechanical and thermal properties such as flexural modulus, flexural strength, heat distortion temperature, Izod im-

Correspondence to: M. Fujiyama (m-fujiyama@tokuyama.co.jp).

Journal of Applied Polymer Science, Vol. 84, 2142–2156 (2002)

Table I Characteristics of Samples

Catalyst	Sample Name	MFI (g/10 min)	Ethylene Content (wt %)	Isotactic Pentad Fraction	M_n (10^4)	M_w (10^4)	M_z (10^4)	M_{z+1} (10^4)	M_w/M_n	M_z/M_w	M_{z+1}/M_z
A	A-1	0.51	0.31		8.4	57	260	610	6.8	4.5	2.3
	A-2	1.77	0.33	0.951	8.3	40	160	460	4.8	4.0	2.9
	A-3	2.0	0	0.956	7.9	41	170	390	5.2	4.2	2.3
	A-4	4.0	0.35		5.8	32	120	260	5.5	3.8	2.2
	A-5	14.5	0		4.3	23	92	230	5.3	4.1	2.5
	A-6	32.6	0		2.8	17	70	170	6.0	4.2	2.4
B	B-1	0.49	0		8.0	63	210	400	7.9	3.3	1.9
	B-2	1.73	0	0.930	4.6	43	170	330	9.4	3.9	1.9
	B-3	4.0	0		3.5	32	150	290	9.1	4.7	1.9
	B-4	8.9	0		2.8	27	130	280	9.5	4.9	2.2
	B-5	14.7	0		2.7	24	130	260	8.9	5.5	2.0
	B-6	25.1	0		2.4	20	110	260	8.5	5.4	2.4

pact strength, and mold shrinkage were studied. As for structures, crystallinity, the thickness of skin layer, a*-axis-oriented component fraction and crystalline orientation functions were studied. The relations between the structures and properties were also studied.

EXPERIMENTAL

Samples

Preparation

PPs prepared by the $MgCl_2$-supported titanium catalyst and by the $TiCl_3$-type catalyst are called cat.-A PPs and cat.-B PPs, respectively. Table I shows the characteristics of samples used in this study. They are the same ones as used in the previous article.[1] The cat.-A PPs were prepared by use of a $MgCl_2$-supported $TiCl_4$ compound, which is generally used industrially, as the main catalyst, of $AlEt_3$ as the cocatalyst, and of an organic silane compound as the tacticity modifier (external donner). The polymerization was carried out in a medium of propylene monomer at 60–70°C. The MFI (molecular weight) was adjusted by use of hydrogen as the chain transfer. Cat.-B PPs were prepared by use of a general δ-type $TiCl_3$ compound (Solvay-type catalyst) as the main catalyst, of $AlEt_2Cl$ as the cocatalyst, and of an organic ester compound as the tacticity modifier (external donner). The polymerization method is the same as that of cat.-A PPs.

Characterization

The MFI (Melt Flow Index) was measured by use of a melt indexer X416 Type (Takara Thermistor Instruments Co. Ltd., Japan) under a 2160-g load at 230°C according to the ASTM D1238-62T. A-1 and B-1, A-2 and B-2, A-4 and B-3, and A-5 and B-5 have similar MFIs, respectively.

Ethylene content was obtained from the absorbance of the 720 cm^{-1} band in infrared absorption spectrum measured by use of an infrared spectrometer IR-700 Type (JASCO, Japan). A small amount of ethylene is copolymerized in A-1, A-2, and A-4 samples.

The isotactic pentad fraction was obtained from ^{13}C-NMR spectrum measured by the use of a nuclear magnetic resonance spectrometer GSX270WB Type (JEOL, Japan). Representative values of the pentad fraction of samples are shown in Table I. cat.-A PPs have pentad fractions about 0.02 higher than those of cat.-B PPs. A-3 of high rigidity grade has a pentad fraction further 0.005 higher than those of the other cat.-A PPs.

Molecular weight distribution was measured with a gel permeation chromatography apparatus GPC150-C Type (Waters Ltd., USA) by use of a column system of 10^3, 10^4, 10^5, 10^6, and 10^7 Å and of *o*-dichlorobenzene as solvent. Figure 1 shows the changes of various molecular weight distribution parameters with MFI. M_w/M_n, a parameter of molecular weight distribution, scarcely depends on MFI for both series of PPs, and their values are 5.5 and 9 for cat.-A PPs and cat.-B PPs, respectively, the former being lower than the lat-

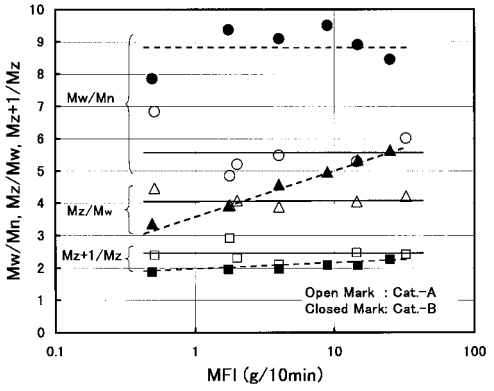

Figure 1 Changes of various molecular weight distribution parameters with melt flow index (MFI).

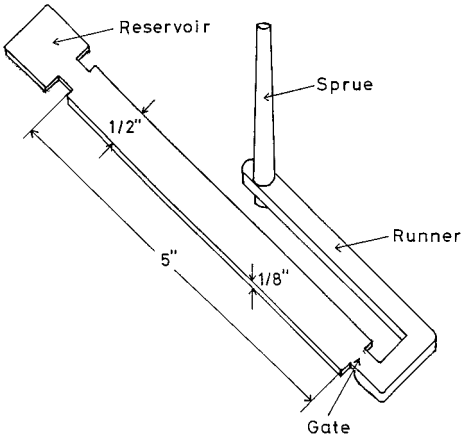

Figure 3 Shape of test specmen.

ter. M_z/M_w, a parameter of molecular weight distribution at the high molecular weight region, increases with increasing MFI for cat.-B PPs, whereas it scarcely depends on MFI for cat.-A PPs.

The crystallization temperature T_c was measured using a differential scanning calorimeter DSC-IB (Perkin-Elmer, USA). A 0.3 mm-thick sheet was molded on a hot plate. A piece weighing about 5 mg was cut out from it. This was put into a sample pan, and after it was melted in the furnace of the DSC in a nitrogen atmosphere at 230°C for 10 min, it was cooled at various rates. The peak temperature of the exothermic curve was taken as T_c. Figure 2 shows the dependence of T_c on cooling rate. Cat.-A PPs show higher T_c than cat.-B PPs. This is due to the higher tacticity of the former, as shown in Table I. Low T_cs of A-1, A-2, and A-4 are due to the copolymerization of small amount of ethylene. Although cat.-B PPs except for B-6 show a similar T_c, only B-6 shows a high T_c nearly equivalent to those of cat.-A PPs copolymerized with a small amount of ethylene. This reason is not clear. T_c lowers with an increase in cooling rate. Comparing the dependence of T_c on the cooling rate between both series of PPs, cat.-A PPs show a slightly weaker dependence than cat.-B PPs, whose reason is also unknown.

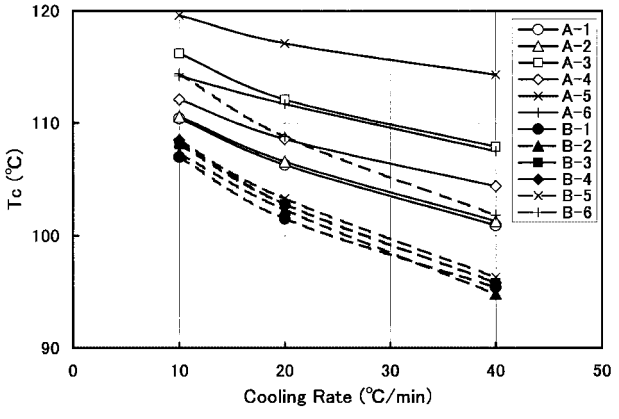

Figure 2 Dependence of crystallization temperature T_c on cooling rate.

Injection Molding

Flexural test specimens (ASTM D790) were injection molded using a reciprocating-screw injection-molding machine SN150S-N Type (clamping force: 150T, capacity: 6.5 oz, Niigata Tekkosho Co., Ltd., Japan). The shape of the test specimen is shown in Figure 3. A polymer reservoir was provided to make resin flow in the specimen uniform. Because cylinder temperature affects the degree of molecular orientation of the product and its mechanical properties more than any other injection molding conditions,[2] injection molding was carried out, varying cylinder temperature only and keeping all other conditions constant. Table II lists the injection molding conditions adopted. For cylinder temperature, the temperature of the metering zone (C_3) at the extreme end was used.

Measurements of Properties

After flexural and Izod test specimens were conditioned under a constant temperature and humidity at 23°C and 50 %RH for 1 month, flexural modulus and flexural strength were measured according to the ASTM D790. Heat distortion

Table II Injection Molding Conditions

Exp. No.	Cylinder Temperture (°C)				Injection Speed (cm^3/s)	Holding Pressure (MPa)	Mold Temperature (°C)	Cooling Time (s)
	C_1[a]	C_2[b]	C_3[c]	N[d]				
1	160	190	200	190	13.5	50	40	40
2	160	220	240	220	13.5	50	40	40
3	160	250	280	250	13.5	50	40	40
4	160	280	320	280	13.5	50	40	40

[a] Feed zone.
[b] Compression zone.
[c] Metering zone.
[d] Nozzle.

temperature was measured under a constant stress of 0.45 MPa according to the ASTM D648. Izod impact strength was measured with molded-in notched specimens according to the ASTM D256. Length L in the flow direction (MD) of the flexural specimen was measured with a micrometer and mold shrinkage was calculated by the following equation:

$$\text{Mold Shrinkage } (\%) = \frac{L_0 - L}{L_0} \times 100 \qquad (1)$$

where L_0 is the length of the mold cavity.

Structural Analysis

A thin section about 0.1 mm-thick was sliced from the central part of the specimen perpendicular to the MD with a microtome, and its crystalline texture was observed with a polarizing microscope PM-6 Type (Olympus, Japan) under a magnification of 20×. Clear skin/core structures were observed for all specimens. The thicknesses of the skin layers of both surfaces were averaged.

Wide-angle X-ray diffraction was carried out at the central part of the specimen with an X-ray diffractometer RU-200 Type (Rigaku Denki, Japan) using a sample spinner and the crystallinity, X_c was calculated according to the Weidinger and Hermans' method.[3] Using a goniometer, 2θ scan was carried out at a scan speed of 4°/min and azimuthal scans of the (110) and (040) plane reflections were carried out at a scan speed of 8°/min, and crystalline orientation functions f_{a^*}, f_b, and f_c were calculated according to the Wilchinsky's method.[4] a*-Axis-oriented component fraction [A^*] was obtained by the method described in the previous articles.[5–12]

These measurements were carried out for all specimens molded from all PP samples at all cylinder temperatures.

RESULTS AND DISCUSSION

Product Properties

Figure 4(a) and (b) shows the dependence of flexural modulus on cylinder temperature for cat.-A PPs and cat.-B PPs, respectively. The result of B-2 sample as a representative of cat.-B PPs is also shown in Figure 4(a) of the results for cat.-A PPs for comparison. The same procedure will be performed in the following results. Although the flexural strength was also measured, it was omitted because it showed a similar behavior to the flexural modulus. The flexural modulus and strength decrease with increasing cylinder temperature. The degree of the decrease is the higher at the lower cylinder temperature, and the decrease tends to level off at high cylinder temperatures. This tendency becomes more notable with increasing the MFI or with decreasing the molecular weight. It is particularly notable for A-6 sample whose flexural modulus and strength scarcely depend on cylinder temperature. Comparing at the same cylinder temperature, the sample with the lower MFI or with the higher molecular weight shows the higher flexural modulus and strength as a large tendency. However, the order reverses in part at high cylinder temperatures, and the sample with the higher MFI shows the higher flexural modulus and strength. The dependence of flexural modulus and strength on MFI is more notable for cat.-A PPs than for cat.-B PPs. Compared at the same cylinder temperature and

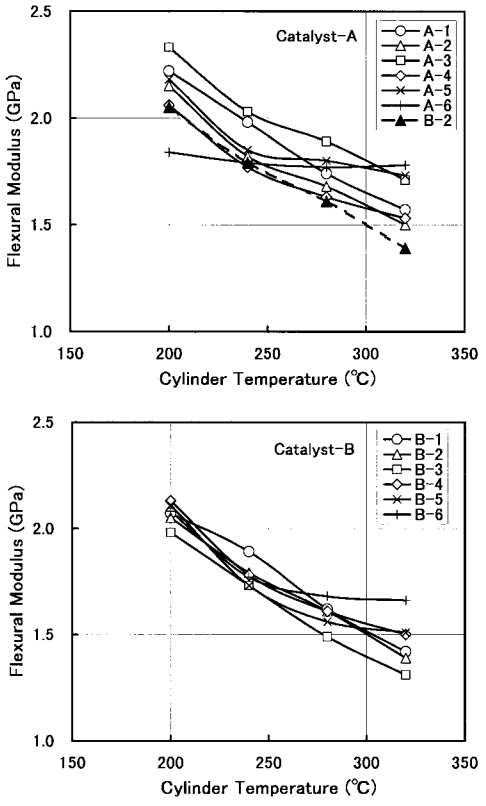

Figure 4 (a) Dependence of flexural modulus on cylinder temperature for cat.-A PPs. (b) Dependence of flexural modulus on cylinder temperature for cat.-B PPs.

MFI, cat.-A PPs show higher flexural modulus and strength than cat.-B PPs. This is due to the higher tacticity of the former, as shown in Figure 2 and Table I. The A-3 sample with particularly high tacticity among cat.-A PPs shows particularly high flexural modulus and strength. The reason why the MFI dependence of flexural modulus and strength of cat.-A PPs is more notable than that of cat.-B PPs is because the MFI dependence of molecular orientations such as the thickness of skin layer and the degree of crystalline orientation is weaker for the latter, as shown later. This is due to the fact that the MFI dependence of the relaxation time of melt orientation, λ_0, is weaker for the latter as shown in Figure 5, whose primary cause is that M_z/M_w, a parameter of molecular weight distribution at high molecular weight region, increases with increasing MFI for the latter, whereas it scarcely depends on MFI for the former, as shown in Figure 1. Both figures were presented in the previous artricle.[1]

The fact that the flexural modulus and strength of injection-molded PP decrease with increasing cylinder temperature is already reported by the authors for homo PPs,[2,13–15] PP copolymers with ethylene,[16,17] α-crystal nucleator-added PPs,[7] β-crystal nucleator-added PPs,[18,19] polystyrene (PS)-blended PPs,[12] particulate-filled PPs,[5,10,11] and glass fiber (GF)-filled PPs,[20] and by other researchers,[21,22] and is considered to be a common knowledge. Song et al.[23] injection molded PPs at high speed, high pressure, and low resin temperature (165–190°C) to prepare a self-reinforced PP by injection molding, and found that the flexural modulus and strength increase with increasing the resin temperature and decrease after showing a peak. This is the inverse tendency of the common knowledge, and is considered to be a special case. The fact that the flexural modulus and strength increase with decreasing the MFI or with increasing the molecular weight is reported by the authors.[2,13–15] In the study of the self-reinforced PP by Song et al.[23] mentioned above, while the flexural modulus and strength of conventionally injection-molded PPs scarcely depend on the weight-average molecular weight M_w, those of the self-reinforced PP moldings show maxima at an M_w of 4.7×10^5. As for the effect of molecular weight distribution, Tartari and Bramuzzo[24] and Hebert[25] report that the flexural modulus is higher as the molecular weight distribution is broader. As for the effect of tacticity, Phillips et al.[26] report that the flexural modulus is enhanced with increasing tacticity due to the increased crystallinity. Phillips et al.[26] and Hayashi and Kimoto[27] report that the flexural modulus of injection-molded PP is mainly determined by the degree of molecular orientation and crystallinity, and is higher as both are higher. Phillips et al. succeeded in the separation

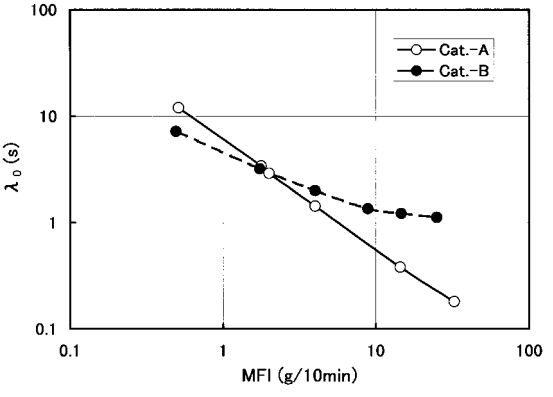

Figure 5 Relation between characteristic relaxation time λ_0 and melt flow index (MFI).

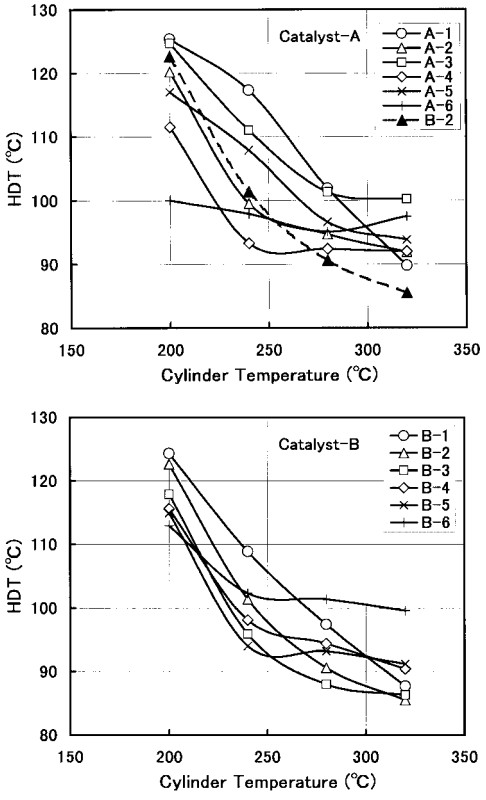

Figure 6 (a) Dependence of heat distortion temperature (HDT) on cylinder temperature for cat.-A PPs. (b) Dependence of heat distortion temperature (HDT) on cylinder temperature for cat.-B PPs.

of the both effects. This will be discussed again later.

Figure 6(a) and (b) shows the dependence on cylinder temperature of heat distortion temperature HDT, which is a measure of heat resistance for cat.-A PPs and cat.-B PPs, respectively. Similar behaviors to the cases of flexural modulus and strength are observed. Because HDT is the temperature when the deformation under a constant stress reaches a definite value, it is higher as the modulus at high temperatures is higher. Accordingly, the result mentioned above is natural. The leveling off of the decrease in HDT with cylinder temperature at high cylinder temperatures is more notable than those in flexural modulus and strength.

The fact that the HDT of injection-molded PP decreases with increasing cylinder temperature is reported by the authors for PP copolymers with ethylene,[16,17] α-crystal nucleator-added PPs,[7] β-crystal nucleator-added PPs,[18,19] PS-blended PPs,[12] and particulate-filled PPs.[10] No study of the dependence of HDT on MFI or molecular weight is found by the authors. The effects of molecular weight distribution and tacticity are also not reported. The effects of molecular weight, its distribution, and tacticity on the HDT of injection-molded PP are reported first in the present study.

Figure 7(a) and (b) shows the dependence of Izod impact strength IIS on cylinder temperature for cat.-A PPs and cat.-B PPs, respectively. IIS decreases with increasing MFI and cylinder temperature. Almost no difference in these behaviors between both series of PPs is observed. Although the flexural modulus and strength and HDT decrease with increasing MFI as a large tendency, some indentations exist in the orders when viewed individually. However, IIS is aligned in the order of MFI. The decrease in IIS with increasing cylinder temperature from 200 to 320°C is 20–30%, which is nearly the same degree as those in flexural modulus and strength. However, the decrease in IIS with increasing MFI is very marked compared with those in flexural modulus and strength. Generally, the impact strengths of

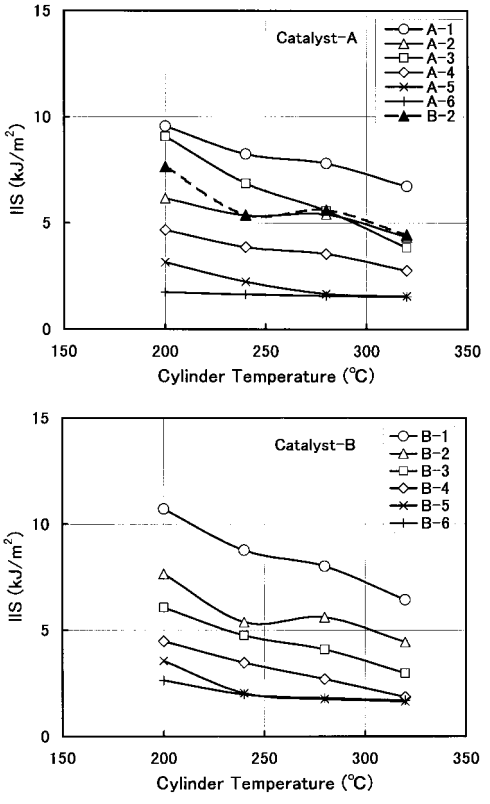

Figure 7 (a) Dependence of Izod impact strength (IIS) on cylinder temperature for cat.-A PPs. (b) Dependence of Izod impact strength (IIS) on cylinder temperature for cat.-B PPs.

thermoplastics increase with increasing the molecular weight. Furthermore, because IIS decreases with increasing cylinder temperature or with decreasing the degree of molecular orientation, IIS is assumed to also be affected by the molecular orientation. In addition, the crystallinity may also affect IIS in some way. From the facts that IIS decreases largely and finely with increasing MFI and that the degree of molecular orientation does not show such remarkable MFI dependence as mentioned later, it is assumed that IIS is determined mainly by the strength of resin itself.

The fact that the IIS of injection-molded PP decreases with increasing cylinder temperature is reported by the authors for PP copolymers with ethylene,[16,17] α-crystal nucleator-added PPs,[7] β-crystal nucleator-added PPs,[18,19] PS-blended PPs,[12] and particulate-filled PPs.[10] Kantz et al.[21] also report a similar result for a homo PP. However, an inverse tendency that IIS increases with increasing cylinder temperature is also reported.[22,28] As for the effect of MFI on IIS, Murphy et al.[29] report an inverse result that IIS decreases with decreasing MFI. The fact that inverse results are obtained in the effects of cylinder temperature and MFI on IIS and not common is assumed to be due to the differences among the reported studies in the shape of molding, the molding conditions, the test direction, and the notching method (molded-in notch in the present experiment). As for the effect of molecular weight distribution, Altendorfer and Seitl[30,31] report that the IISs of controlled rheology PPs with narrow molecular weight distributions are higher than those of usual PPs compared at the same MFI. Tartari and Bramuzzo[24] and Hebert[25] show that IIS is generally lower as the molecular weight is broader. No study is reported on the effect of tacticity.

Figure 8(a) and (b) show the dependence of mold shrinkage on cylinder temperature for cat.-A PPs and cat.-B PPs, respectively. Mold shrinkage decreases with increasing MFI and cylinder temperature. The MFI dependence of mold shrinkage of cat.-A PPs is more notable than that of cat.-B PPs. This is due to the fact that the MFI dependence of the relaxation time of melt orientation, λ_0, is weaker for the latter, as shown in Figure 5, whose primary cause is that M_z/M_w, a parameter of molecular weight distribution at high molecular weight region, increases with increasing MFI for the latter, whereas it scarcely depends on MFI for the former, as shown in Figure 1. From the facts that the mold shrinkage finely aligns in the order of MFI and that the MFI dependence of mold shrinkage is very similar to that of the degree of molecular orientation as shown later, it is assumed that the mold shrinkage is most affected by the molecular orientation. Although both the IIS and mold shrinkage similarly finely align in the order of MFI, their causes are different; the former is due to the strength of resin itself and the latter is due to the molecular orientation. Contrary to this, because the flexural modulus and strength and HDT do not finely align in the order of MFI and because these properties level off at high cylinder temperatures and there are cases where a high MFI resin shows high properties, it is assumed that these properties are considerably affected also by crystallinity.

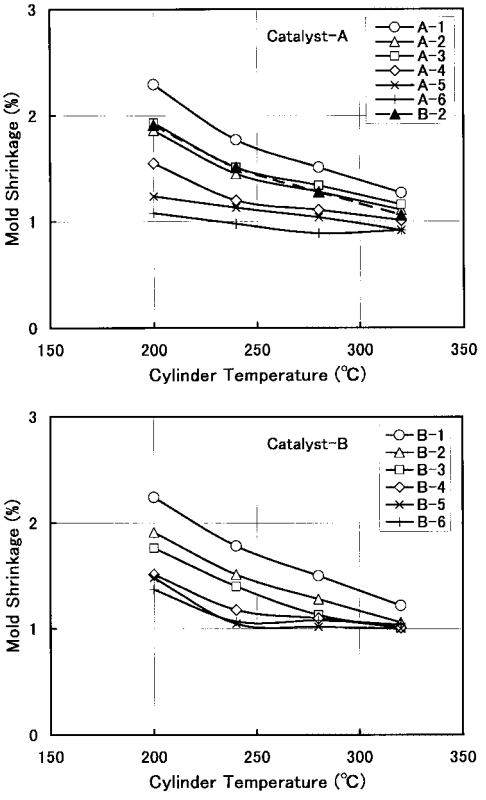

Figure 8 (a) Dependence of mold shrinkage on cylinder temperature for cat.-A PPs. (b) Dependence of mold shrinkage on cylinder temperature for cat.-B PPs.

The fact that the mold shrinkage of injection-molded PP decrease with increasing cylinder temperature is already reported by the authors for homo PPs,[2] PP copolymers with ethylene,[16,17] α-crystal nucleator-added PPs,[7] β-crystal nucleator-added PPs,[18,19] PS-blended PPs,[12] particulate-filled PPs,[5,11] and GF-filled PPs.[20] Kantz et al.[21]

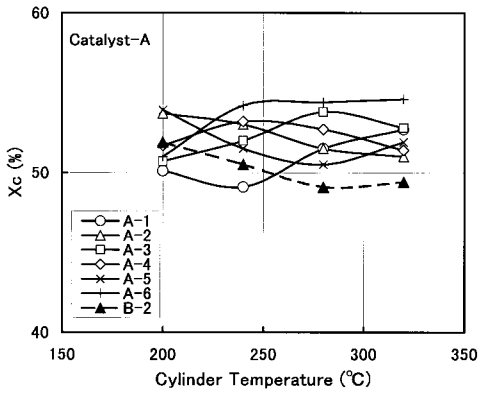

Figure 9 Dependence of degree of crystallinity X_c on cylinder temperature for cat.-A PPs.

and Plessmann et al.[32] also report similar results. The fact that the mold shrinkage decreases with increasing MFI is shown by the authors,[2,33] and the fact that it is higher as the molecular weight distribution is broader is also shown by the authors.[33] No report on the effect of tacticity is found.

Higher Order Structure

Figure 9 shows the dependence of crystallinity X_c on cylinder temperature for cat.-A PPs. X_c scarcely depends on MFI and cylinder temperature. Similar results were also obtained for cat.-B PPs. The mean values of X_c averaged over all specimens are 52.2 and 51.1% for cat.-A PPs and cat.-B PPs, respectively, the former being about 1.1% higher. The A-3 sample with high tacticity and rigidity does not entirely show particularly high X_c, and shows similar X_c value to those of other cat.-A PPs. However, A-6 and B-6 samples that show particularly high crystallization temperatures T_c and particularly remarkable leveling-off of the properties at high cylinder temperatures in each catalyst system show high X_c at high cylinder temperatures.

The authors report that X_cs of PP copolymers with ethylene[16] scarcely depend on cylinder temperature and X_cs of homo PPs,[8] α-crystal nucleator-added PPs,[7] PS-blended PPs,[12] particulate-filled PPs[9] slightly increase with increasing cylinder temperature. Yang and Nun[34] also obtained similar results. Murphy et al.[28] obtained an inverse result that X_c decreases with increasing cylinder temperature. As for the effect of MFI, that X_c slightly increases with increasing MFI is reported by the authors.[8] Murphy et al.[29] obtained an inverse result. No study is reported on the effect of molecular weight distribution. Phillips et al.[26] report that X_c is the higher as the tacticity is the higher. The experimental results in the present study are generally on the same line of these previous findings in the sense of little MFI dependence.

All specimens molded in the present study showed clear skin/core structures. Figure 10(a) and (b) shows the dependence of thickness of the kin layer on cylinder temperature for cat.-A PPs and cat.-B PPs, respectively. The skin thickness decreases with increasing MFI and cylinder temperature. The MFI dependence of skin thickness of cat.-A PPs is more notable than that of cat.-B PPs.

The skin layer in injection molding develops by cooled solidification under a shear stress of flow in the mold cavity,[35–38] and its formation is determined by the degree of melt orientation of molecular chains by the action of shear stress (recoverable shear strain γ_e), the rate of its relaxation (relaxation time λ_0), and the time until solidification (crystallization time t_c or crystallization tem-

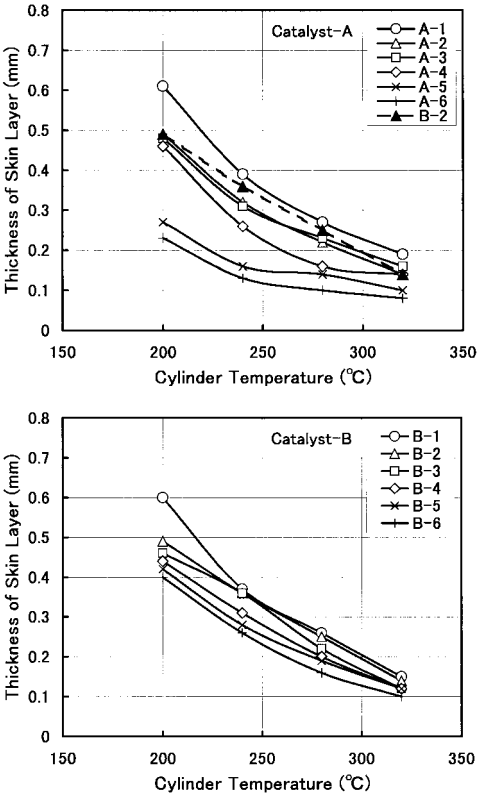

Figure 10 (a) Dependence of thickness of skin layer on cylinder temperature for cat.-A PPs. (b) Dependence of thickness of skin layer on cylinder temperature for cat.-B PPs.

perature T_c).[2,8,9,10,11,14,15,20,33,39–42] The higher γ_e, the longer λ_0, and the shorter t_c or the higher T_c, the thicker the skin layer. At first as for the effect of cylinder temperature, the higher the cylinder temperature, the higher the resin temperature and then the lower γ_e and the shorter λ_0, which leads the thinner skin layer. As for the effect of MFI, the higher MFI at the same cylinder temperature (at the same t_c), the lower γ_e and the shorter λ_0, which leads the thinner skin layer. The difference in MFI dependence of skin thickness between cat.-A PPs and cat.-B PPs is due to the fact that the MFI dependence of the relaxation time of melt orientation, λ_0, is weaker for the latter as shown in Figure 5, whose primary cause is that M_z/M_w, a parameter of molecular weight distribution at high molecular weight region, increases with increasing MFI for the latter, whereas it scarcely depends on MFI for the former as shown in Figure 1. It can be said from this that the skin thickness is affected by both the molecular weight M_w and the molecular weight distribution at high molecular weight region, M_z/M_w, and becomes thicker as the both become higher. As for the effect of tacticity, because the crystallization temperature T_c becomes higher, and hence, the crystallization time t_c becomes shorter when the tacticity becomes higher as shown in Figure 2, it is predicted that the skin thickness becomes thicker as the tacticity becomes higher. However, Figure 10 shows that its effect is small.

The fact that the skin thickness of injection-molded PP decreases with increasing cylinder temperature is already reported by the authors for homo PPs,[2,8,11,13–15,33,43,44] PP copolymers with ethylene,[11,16,17,44] β-crystal nucleator-added PPs,[18,19] particulate-filled PPs,[5,9–11] and GF-filled PPs,[20] and by other researchers,[21,26,32,38,45–48] and is considered to be common knowledge. The fact that the skin thickness decreases with increasing the MFI or with decreasing the molecular weight is reported by the authors[2,8,11,13–15,33,43,44,49] and by other researchers.[26,48] The fact that the skin layer is thicker as the molecular weight distribution is broader is shown by the authors[33,49] and by other researchers[26,30,31,45,50,51] mainly by use of controlled rheology PPs. As for the effect of tacticity, Phillips et al.[26] showed that it scarcely affects the skin thickness as in the case of the present study.

Figure 11 shows the dependence of a*-axis-oriented component fraction [*A**] on cylinder temperature. [*A**] increases with increasing cylinder temperature and MFI. The dependence of [*A**] on cylinder temperature is stronger for cat.-A PPs than for cat.-B PPs. This tendency is reverse of the tendency of the skin thickness for its dependence on MFI and cylinder temperature, and is the same for the degree of MFI dependence. Accordingly, it is assumed that [*A**] is affected by the molecular weight distribution at the high molecular weight region, M_z/M_w, as well as the molecular weight M_w. It is higher as both are lower, meaning that the a*-axis-oriented component against the c-axis-oriented component is higher. [*A**] in the present experiment is higher than 0.7, which means that the a*-axis-oriented component is overwhelmingly more than the c-axis-oriented component in injection-molded PPs. This tendency becomes more remarkable as a resin with high MFI and narrow molecular weight distribution is molded at high cylinder temperature. The effect of tacticity is not clear.

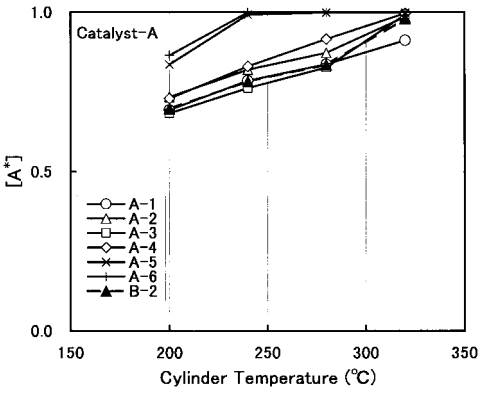

Figure 11 Dependence of a*-axis-oriented component fraction [*A**] on cylinder temperature for cat.-A PPs.

As far as the authors know, the study of a*-axis-oriented component fraction [*A**] has only been done by us. The fact that [*A**] of injection-molded PP increases with increasing the cylinder temperature is already reported by the authors for homo PPs,[8,11] PP copolymers with ethylene,[16] α-crystal nucleator-added PPs,[7] PS-blended PPs,[12] particulate-filled PPs,[5,9,10] and GF-filled PPs.[20] The fact that [*A**] increases with increasing MFI is also shown by the authors.[8] The present study is the first that reports the effect of molecular weight distribution.

Figure 12(a) and (b) shows the dependence of crystalline orientation functions (a*-axis orientation function f_{a^*}, b-axis orientation function f_b, and c-axis orientation function f_c) on cylinder

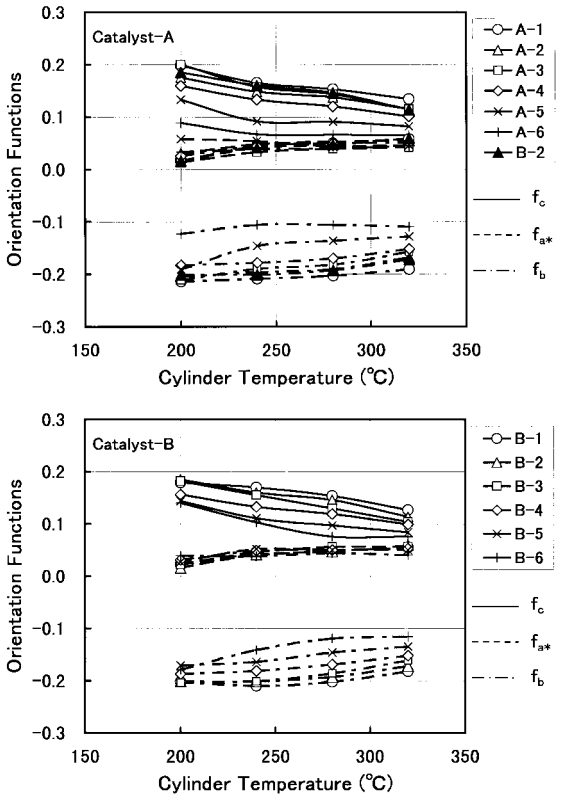

Figure 12 (a) Dependence of orientation functions on cylinder temperature for cat.-A PPs. (b) Dependence of orientation functions on cylinder temperature for cat.-B PPs.

temperature for cat.-A PPs and cat.-B PPs, respectively. Absolute values of f_c and f_b decrease with increasing cylinder temperature and MFI. The dependence of absolute values of f_c and f_b on MFI is stronger for cat.-A PPs than for cat.-B PPs. f_{a^*} scarcely depends on MFI, and increases with increasing the cylinder temperature. Because the c-axis orientation function in the direction of crystalline molecular chains is usually used as a measure of degree of crystalline orientation, the following discussion will be done for f_c. As for the formation of crystalline orientation, the same discussion as done on the skin thickness is used as such. Namely, it can be explained by the recoverable shear strain γ_e, its relaxation time λ_0, and the crystallization time t_c. Accordingly, the effects of cylinder temperature and MFI on the crystalline orientation function are omitted, and only the fact characteristic in the present study that the dependence of the orientation function on MFI is stronger for cat.-A PPs than for cat.-B PPs will be referred. This reason is because the MFI dependence of λ_0 is weaker for the latter because M_z/M_w increases with increasing MFI for the latter, whereas it scarcely depends on MFI for the former. The similarity of formation mechanisms of the skin layer and the crystalline orientation is obvious by considering the intimate relationship existing between the skin thickness and the crystalline orientation function f_c.[5,15,26]

The fact that the degree of crystalline orientation of injection-molded PP decreases with increasing cylinder temperature is already reported by the authors for homo PPs,[8,11,14,15] PP copolymers with ethylene,[11,16,17] α-crystal nucleator-added PPs,[7,11] PS-blended PPs,[12] particulate-filled PPs,[5,9] and GF-filled PPs.[11,20] Other researchers[26,28,47,51,54] also obtained similar results. The fact that the degree of crystalline orientation decreases with increasing the MFI or with decreasing the molecular weight is reported by the authors[8,11,14,15] and by other researchers.[26,29] The fact that the degree of crystalline orientation is higher as the molecular weight distribution is broader[24,26,30,31,50–52,55] is shown mainly by use of controlled rheology PPs.[30,31,50–52,55] As for the effect of tacticity, Phillips et al.[26] showed that it scarcely affects the degree of crystalline orientation as in the case of the present study.

In injection molding of thermoplastics, because molten resin solidifies under inhomogeneous stress and cooling conditions, the inner structures of the molded article are inhomogeneous, influencing the product properties. Consequently, it is important in injection molding technology of thermoplastics to clarify the influences of the primary structures of resin and molding conditions on the inhomogeneous structure of the molded article. We studied the distributions in the flow direction of higher order structures such as thickness of skin layer, a*-axis-oriented component fraction, and crystalline orientation functions and distributions in the thickness direction of higher order structures such as crystallinity, β-crystal content, a*-axis-oriented component fraction, and crystalline orientation functions in injection moldings molded from the both series of PPs. However, no remarkable difference was detected between them.

Structure–Property Relationship

Various higher order structures, such as skin/core structure, orientations of molecular chains and crystallites, spherulite size, lamella thickness, crystallinity, length and orientation of filled fi-

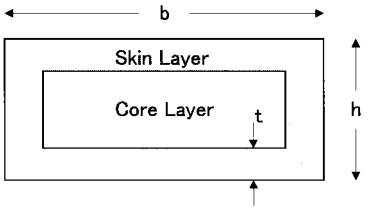

Figure 13 Two-phase model of skin and core.

bers, are formed according to the characteristics of raw resin and molding conditions in injection-molded PPs, which determines the product properties.[56] Accordingly, it is important in molding technology to clarify the relationship among raw resin–molding conditions–higher order structures–product properties. Here, giving attention to the skin thickness and crystalline orientation out of the higher order structures mentioned above, with also considering crystallinity if necessary, the relationships between the structures and properties are studied.

When observed with a polarizing microscope, the cross-section of an injection-molded article shows a skin/core structure, and the two-phase model of skin and core shown in Figure 13 can be applied. In Figure 13, b and h are, respectively, the width and thickness of the specimen and t is the thickness of skin layer. If, in this two-phase model, E is the flexural modulus of the whole, E_s and E_c are the flexural moduli of, respectively, the skin and core layers, the following equation holds:[2,5,11,14–17]

$$E = E_s - \frac{(E_s - E_c)}{bh^3}\{(b - 2t)(h - 2t)^3\} \quad (2)$$

If E is plotted against $(b-2t)(h-2t)^3$ with respect to specimens with different values of t prepared at various cylinder temperatures, a rectilinear relationship can be obtained, and E_s can be obtained from an E-axis intercept and E_c can be obtained from the slope. Figure 14 shows such plots for cat.-A PPs. In the case of cat.-B PPs, while such rectilinear relationships were obtained for B-1 and B-2 samples, downward-curved relationships with negative slopes were obtained for other samples. Compared at the same skin thickness, the flexural moduli of cat.-A PPs are higher than those of cat.-B PPs. Compared among cat.-A PPs, A-1, A-2, and A-4 samples, which are copolymerized with small amounts of ethylene, show lower flexural moduli than A-3, A-5, and A-6 samples without ethylene. The A-3 sample with particularly high tacticity out of cat.-A PPs without ethylene does not show particularly high flexural modulus. If the skin thickness is regarded as a measure of molecular orientation, plots of property values against the skin thickness as in Figure 14 can make one separate the effect of the skin thickness (molecular orientation) on the property from the effect of other structural factors and evaluate them individually. Namely, that the position of the relation curve (straight line in the case of Fig. 14) of the property value vs. the skin thickness is higher on the property value-axis means that the effect of structural factors other than the skin thickness is stronger. Because the structural factors affecting the flexural modulus of injection-molded PPs are the degree of molecular orientation and crystallinity,[11,26,56] the position of the relation line in Figure 14 may be regarded mainly as the effect of cryatallinity. As mentioned previously in relation to Figure 9, there is a difference of about 1.1% in average crystallinity X_c between cat.-A PPs and cat.-B PPs, which agrees with the tendency in Figure 14. However, there is no clear correlation between the crystallinities in Figure 9 and the positions of the relation lines in Figure 14 for the same catalyst system's PPs. Rather, a good correlation is observed between the crystallization temperatures T_c in Figure 2 and the positions of the relation lines in Figure 14 (including the case of cat.-B PPs whose figure is not shown). The higher T_c leads the higher flexural modulus at a constant skin thickness. Generally, the crystallinity of PP is higher as the tacticity is higher, and is lowered by the copolymerization with ethylene.[11,26] This tendency is clearly observed on the crystallization temperature T_c in Figure 2 and on the flexural

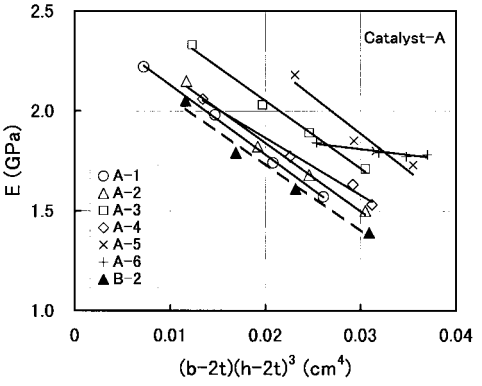

Figure 14 Plot of flexural modulus E against $(b-2t)(h-2t)^3$ for cat.-A PPs.

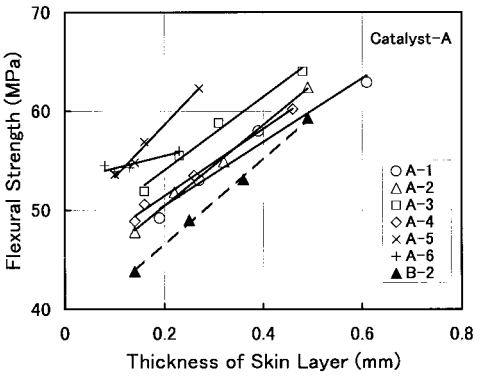

Figure 15 Relation between flexural strength and thickness of skin layer for cat.-A PPs.

modulus in Figure 14. However, it is not clearly reflected to the crystallinity X_c in Figure 9. From this, it may be said that the measurement of the crystallinity X_c by X-ray diffraction is not as good in the precision and not suitable to the detection of small difference in crystallinity. The small difference in the crystallinity may be able to be sensitively detected rather by T_c and mechanical properties.

The relations between the flexural (tensile) modulus and the skin thickness are studied by the authors for homo PPs[2,13–15,43,49] (the effects of molecular weight distribution and tacticity are not studied), PP copolymers with ethylene,[16,17] particulate-filled PPs,[5,10] and GF-filled PPs,[20] and by other researchers,[22,26] and similar results are obtained. Phillips et al.[26] separated the effect of crystallinity on the flexural modulus from the effect of the skin thickness and corrected the flexural modulus by the crystallinity. As a result, they showed that the relation between the corrected flexural modulus and the skin thickness is expressed by a master straight line independent of the kind of resin (differing in tacticitiy and MFI) and molding conditions.

Figure 15 shows the relation between the flexural strength and the skin thickness for cat.-A PPs. The flexural strength increases linearly with increasing skin thickness. Similarly to the case of the flexural modulus, while rectilinear relationships were obtained for B-1 and B-2 samples, downward-curved relationships with positive slopes were obtained for other cat.-B PP samples. The relation between the flexural strength and the skin thickness can be similarly discussed to the case of flexural modulus. The relations between the flexural (tensile) strength and the skin thickness are studied by the authors for homo PPs[2,13–15,43,49] (the effects of molecular weight distribution and tacticity are not studied), PP copolymers with ethylene,[16,17] particulate-filled PPs,[5,10] and GF-filled PPs,[20] and by Kantz et al.[21] for a homo PP and a copolymer, and similar results are obtained.

Figure 16 shows the relation between the heat distortion temperature HDT and the skin thickness. The HDT rises curvilinearly with increasing skin thickness. Cat.-B PPs also show a similar tendencies. Except that the relation is curvilinear, the HDT behaves similarly to the flexural modulus and strength. Accordingly, the HDT also can be similarly discussed to the flexural modulus and strength. Namely, the heat resistance of injection-molded PP is improved by molding it as the skin layer becomes thicker: by molding a resin with low MFI or high molecular weight and with broad molecular weight distribution at a low cylinder temperature. Using a resin with high tacticity and without copolymerized ethylene is also effective. The relations between the HDT and the skin thickness are studied by the authors for PP copolymers with ethylene,[16,17] particulate-filled PPs,[5,10] and GF-filled PPs,[20] and similar results (correlationships between the both) are obtained.

Figure 17 shows the relation between the Izod impact strength (IIS) and the skin thickness for cat.-A PPs. The IIS slightly increases linearly with increasing skin thickness. Compared at the same skin thickness, the lower the MFI or the higher the molecular weight, the higher the IIS. Similar results were obtained also for cat.-B PPs. Cat.-A PPs and cat.-B PPs show similar IISs at the same MFI and at the same skin thickness. From this, it is assumed that the effect of tacticity on IIS is small in the tacticity range of the samples used in the present study. The relations be-

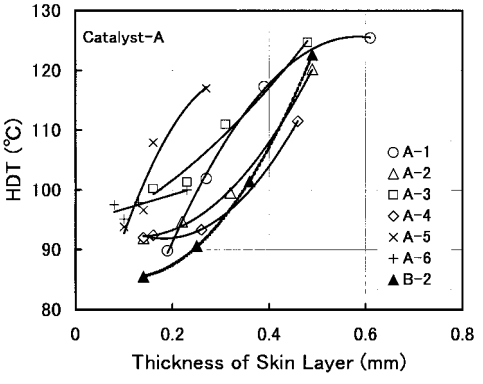

Figure 16 Relation between heat distortion temperature (HDT) and thickness of skin layer for cat.-A PPs.

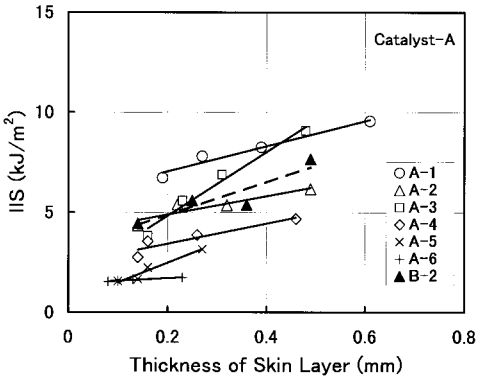

Figure 17 Relation between Izod impact strength (IIS) and thickness of skin layer for cat.-A PPs.

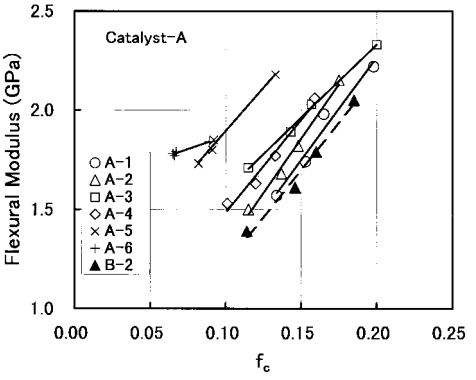

Figure 19 Relation between flexural modulus and c-axis orientation function f_c for cat.-A PPs.

tween the IIS and the skin thickness are studied by the authors for PP copolymers with ethylene,[16,17] particulate-filled PPs,[5,10] and GF-filled PPs,[20] and by Kantz et al.[21] for a homo PP, and similar results (correlationships between the both) are obtained. However, Cunha et al.[22] report an inverse result that the IIS decreases with increasing the skin thickness. The cause that the inverse relations between the IIS and the skin thickness are obtained is assumed to be due to the differences in the shape of test specimen, notching manner, test direction, etc. In this connection, molded-in notched IIS specimens were tested in the transverse direction to the flow direction (MD) in the present experiment.

Figure 18 shows the relation between the mold shrinkage and the skin thickness for cat.-A PPs. The flexural strength increases linearly with increasing skin thickness. Compared at the same skin thickness, while the lower the MFI or the higher the molecular weight, the slightly higher the mold shrinkage. Similarly to the cases of the flexural modulus and strength, while rectilinear relationships were obtained for B-1 and B-2 samples, downward-curved relationships with positive slopes were obtained for other cat.-B PP samples. That the lower the MFI or the higher the molecular weight, the slightly higher the mold shrinkage is the same also for cat.-B PPs. From these, it is assumed that although the mold shrinkage is determined almost by the skin thickness, other factors also partly affect it. From the fact that cat.-A PPs and cat.-B PPs show similar mold shrinkages at the same MFI and at the same skin thickness, it is assumed that the effect of tacticity on the mold shrinkage is small in the tacticity range of the samples used in the present study. The relations between the mold shrinkage and the skin thickness are studied by the authors for homo PPs,[2,33] PP copolymers with ethylene,[16,17] particulate-filled PPs,[5,10,11] and GF-filled PPs,[20] and by other researchers,[21,32] and similar results (correlationships between the both) are obtained.

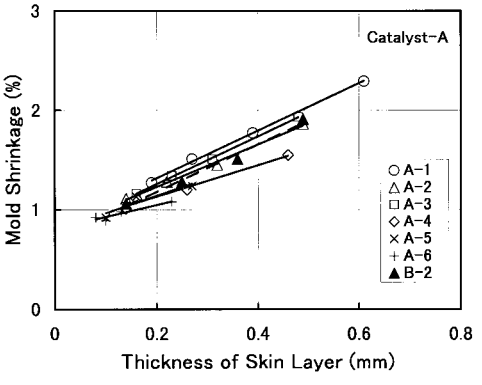

Figure 18 Relation between mold shrinkage and thickness of skin layer for cat.-A PPs.

Next, relations between the properties and the crystalline orientation functions will be studied. The c-axis orientation function f_c in the direction of crystalline molecular chains is used out of the crystalline orientation functions. Figure 19 shows the relation between the flexural modulus and f_c. The flexural modulus increases linearly with increasing f_c. Compared at the same f_c, cat.-A PPs with higher tacticity show higher flexural modulus than cat.-B PPs. A small amount of copolymerization decreases the flexural modulus. These behaviors are almost similar to those in the case of the skin thickness and, hence, the discussion in the case of the skin thickness is applicable as such. The relation between the flexural modulus

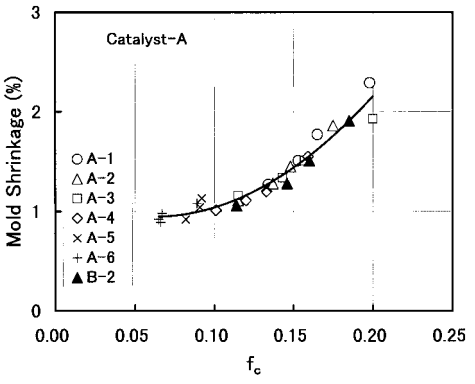

Figure 20 Relation between mold shrinkage and c-axis orientation function f_c for cat.-A PPs.

and f_c was studied by Phillips et al.[26] They separated the effect of crystallinity on the flexural modulus from the effect of the molecular orientation and corrected the flexural modulus by the crystallinity. As a result, they showed that the relation between the corrected flexural modulus and f_c is expressed by a master straight line independent of the kind of resin (differing in tacticitiy and MFI) and molding conditions. Hayashi and Kimoto[27] measured the crystallinities and the degrees of molecular orientation by infrared dichroism for various PPs and found that the flexural modulus can be expressed as a function of the degree of molecular orientation and crystallinity. The present experimental results are on the same line of these previous findings.

The properties other than the flexural modulus also show linear or downward-curved curvilinear relations with positive slopes with f_c, which is similar to that in the case of skin thickness. Individualities of samples remain in the relations between the properties other than mold shrinkage and f_c, and their relations are different for each sample. However, the individualities do not remain in the relation between the mold shrinkage and f_c, and its relation is expressed by a master curve. This relation is shown in Figure 20. From this, it is assumed that the mold shrinkage is determined mainly by the molecular orientation, and the effect of tacticity is very small. Although the individualities of samples that the mold shrinkage slightly increases with decreasing MFI slightly remain in the relation between the mold shrinkage and skin thickness as shown in Figure 18, the individualities are vanished in the relation between the mold shrinkage and f_c as shown in Figure 20. This reason is as follows: although the molecular orientation in injection-molded PPs is condensed mainly in the skin layer, additional molecular orientations exist at parts besides the skin layer,[8,9,11,14,15,26] which also are assumed to affect the mold shrinkage. Although the plots against the skin thickness do not pick up all molecular orientations, the plots against f_c do because f_c is measured throughout the whole thickness direction.

CONCLUSIONS

Two series of PPs with different molecular weight distribution and tacticity characteristics were prepared by the $MgCl_2$-supported catalyst (cat.-A PPs) and by the $TiCl_3$-type catalyst (cat.-B PPs). Flexural test specimens were injection molded from these PPs at cylinder temperatures of 200–320°C and the effects of molecular weight distribution and tacticity on the structure and properties were studied. Measured propertied were flexural modulus, flexural strength, heat distortion temperature, Izod impact strength, and mold shrinkage, and structures studied were crystallinity, the thickness of skin alyer, a*-axis-oriented component fraction, and crystalline orientation functions. The relations between the structures and properties were also studied. The MFI (molecular weight) dependence of the properties is higher for cat.-A PPs than for cat.-B PPs. This originates from weaker MFI dependence of the degrees of molecular orientation such as the skin thickness and the crystalline c-axis orientation function for the latter. This further originates from weaker MFI dependence of the relaxation time of melt orientation for the latter. Its primary cause is that M_z/M_w, a parameter of molecular weight distribution at high molecular weight region, increases with increasing MFI for the latter, whereas it scarcely depends on MFI for the former. Compared at the same skin thickness or c-axis orientation function, cat.-A PPs show higher flexural moduli and strengths and heat distortion temperatures than cat.-B PPs. This is assumed to be due to the higher tacticity and crystallinity for the former. It is said that the molecular weight distribution and tacticity characteristics affect the properties mainly through the molecular orientation and crystallinity, respectively.

The authors would like to thank Tokuyama Corp. for permission to publish this article.

REFERENCES

1. Fujiyama, M.; Kitajima, Y.; Inata, H. J Appl Polym Sci 2002, 84, 2128.
2. Fujiyama, M.; Kimura, S. Kobunshi Ronbunshu 1975, 32, 581.
3. Weidinger, W.; Hermans, P. H. Makromol Chem 1961, 50, 98.
4. Wilchinsky, Z. W. J Appl Phys 1960, 31, 1969.
5. Fujiyama, M.; Kawasaki, Y.; Wakino, T. Nihon Reoroji Gakkaishi 1987, 15, 191.
6. Fujiyama, M.; Wakino, T. ; Kawasaki, Y. J Appl Polym Sci 1988, 35, 29.
7. Fujiyama, M.; Wakino, T. J Appl Polym Sci 1991, 42, 2739.
8. Fujiyama, M.; Wakino, T. J Appl Polym Sci 1991, 43, 57.
9. Fujiyama, M.; Wakino, T. J Appl Polym Sci 1991, 43, 97.
10. Fujiyama, M. Int Polym Process 1992, 7, 358.
11. Fujiyama, M. In Polypropylene: Structure, Blends and Composites: Karger-Kocsis, J., Ed.; Chapman & Hall: London, 1995, p.167.
12. Fujiyama, M. J Appl Polym Sci 1997, 63, 1015.
13. Fujiyama, M.; Awaya, H.; Kimura, S. J Appl Polym Sci 1977, 21, 3291.
14. Fujiyama, M. Nihon Reoroji Gakkaishi 1986, 14, 152.
15. Fujiyama, M. Techno Japan 1986, 19 (11), 28.
16. Fujiyama, M.; Wakino, T. Seikei-Kakou 1991, 3, 217.
17. Fujiyama, M.; Wakino, T. Int Polym Process 1992, 7, 97.
18. Fujiyama, M. Int Polym Process 1995, 10, 172.
19. Fujiyama, M. Int Polym Process 1998, 13, 291.
20. Fujiyama, M. Int Polym Process 1993, 8, 245.
21. Kantz, M. R.; Newman, H. D., Jr.; Stigale, F. H. J Appl Polym Sci 1972, 16, 1249.
22. Cunha, A. M.; Pouzada, A. S.; Oliveira, M. J.; Crawford, R. J. Makromol Chem Macromol Symp 1988, 20/21, 475.
23. Song, J.; Prox, M.; Weber, A.; Ehrenstein, G. In Polypropylene: Structure, Blends and Composites; Karger-Kocsis, J., Ed.; Chapman & Hall: London, 1995, p. 273.
24. Tartari, D.; Bramuzzo, M. Kunststoffe 1993, 83, 460.
25. Hebert, G. SPE Technical Paper 52th ANTEC, 1994, 40, 579.
26. Phillips, R.; Hebert, G.; News, J.; Wolkowicz, M. Polym Eng Sci 1994, 34, 1731.
27. Hayashi, T.; Kimoto, M. Seikei-Kakou 1995, 227.
28. Murphy, M. W.; Thomas, K.; Bevis, M. J. Plast Rubber Process Appl 1988, 9, 3.
29. Murphy, M. W.; Thomas, K.; Bevis, M. J. Plast Rubber Process Appl 1988, 9, 117.
30. Altendorfer, F.; Seitl, E. Plastverarbeiter 1984, 35 (10), 144.
31. Altendorfer, F.; Seitl, E. Kunststoffe 1986, 76, 47.
32. Plessmann, K.; Menges, G.; Cremer, M.; Fenske, W.; Feser, W.; Netze, C.; Offergeld, H.; Pötsch, G.; Stabrey, H. Kunststoffe 1990, 80, 200.
33. Fujiyama, M.; Kimura, S. J Appl Polym Sci 1978, 22, 1225.
34. Yang, T. H.; Nunn, R. E. SPE Technical Paper 50th ANTEC, 1992, 38, 48.
35. Janeschitz-Kriegl, H. Rheol Acta 1977, 16, 327.
36. Janeschitz-Kriegl, H. Rheol Acta 1979, 18, 693.
37. Brito, A. M.; Gunha, A. M.; Pouzada, A. S.; Crawford, R. J. Int Polym Process 1991, 6, 370.
38. Isayev, A. I.; Chan, T. W.; Gmerek, M.; Shimoji, K. J Appl Polym Sci 1995, 55, 821.
39. Fujiyama, M.; Kawasaki, Y.; Wakino, T. Nihon Reoroji Gakkaishi 1987, 15, 203.
40. Fujiyama, M. Nihon Reoroji Gakkaishi 1989, 17, 5.
41. Fujiyama, M.; Wakino, T. Seikei-Kakou 1991, 3, 301.
42. Fujiyama, M.; Wakino, T. Int Polym Process 1992, 7, 159.
43. Fujiyama, M.; Kimura, S. Kobunshi Ronbunshu 1975, 32, 591.
44. Fujiyama, M.; Azuma, K. J Appl Polym Sci 1979, 23, 2807.
45. Koppelmann, J.; Fleischmann, E.; Leitner, G. Rheol Acta 1987, 26, 548.
46. Miyamoto, A.; Matsui, Y.; Uda, T.; Hashimoto, T. Seikei-Kakou 1993, 5, 261.
47. Menges, G.; Ries, H.; Wiegmann, T. Kunststoffe 1987, 77, 433.
48. Guo, X.; Isayev, A. I.; Demiray, M. Polym Eng Sci 1999, 39, 2132.
49. Fujiyama, M.; Kimura, S. J Appl Polym Sci 1977, 21, 2283.
50. Altendorfer, F.; Geymayer, G. Plastverarbeiter 1983, 34(6), 511.
51. Fleischmann, E.; Koppelmann, J. Kunststoffe 1988, 78, 453.
52. Fleischmann, E.; Koppelmann, J. Kunststoffe 1987, 77, 405.
53. Menges, G.; Troost, A.; Koske, J.; Ries, H.; Stabrey, H. Kunststoffe 1988, 78, 806.
54. Fleischmann, E. Int Polym Process 1989, 4, 158.
55. Zipper, P.; Jánosi, A.; Wrentschur, E.; Geymayer, W.; Ingolic, E.; Friesenbichler, W.; Eigl, F. Int Polym Process 1997, 7, 192.
56. Fujiyama, M. In Polypropylene: An A-Z Reference; Karger-Kocsis, J., Ed.; Kluwer Publishers: Dordrecht, 1999, p. 519.